

# Scalable Population Synthesis with Deep Generative Modeling

Stanislav S. Borysov, Jeppe Rich, Francisco C. Pereira

*Department of Management Engineering, Technical University of Denmark, DTU, 2800 Kgs. Lyngby, Denmark*

---

## Abstract

Population synthesis is concerned with the generation of synthetic yet realistic representations of populations. It is a fundamental problem in the modeling of transport where the synthetic populations of micro agents represent a key input to most agent-based models. In this paper, a new methodological framework for how to grow pools of micro agents is presented. This is accomplished by adopting a deep generative modeling approach from machine learning based on a Variational Autoencoder (VAE) framework. Compared to the previous population synthesis approaches based on Iterative Proportional Fitting (IPF), Markov Chain Monte Carlo (MCMC) sampling or traditional generative models, the proposed method allows unparalleled scalability with respect to the number and types of attributes. In contrast to the approaches that rely on approximating the joint distribution in the observed data space, VAE learns its compressed latent representation. The advantage of the compressed representation is that it avoids the problem of the generated samples being trapped in local minima when the number of attributes becomes large.

The problem is illustrated using the Danish National Travel Survey data, where the Gibbs sampler fails to generate a population with 21 attributes (corresponding to the 121-dimensional joint distribution). At the same time, VAE shows acceptable performance when 47 attributes (corresponding to the 357-dimensional joint distribution) are used. Moreover, VAE allows for growing agents that are virtually different from those in the original data but have similar statistical properties and correlation structure. The presented approach will help modelers to generate better and richer populations with a high level of detail, including smaller zones, personal details and travel preferences.

*Keywords:* Population synthesis, Generative modeling, Deep learning, Variational Autoencoder, Transport modelling, Agent-based modelling

---

## 1. Introduction

Population synthesis is a common term for models that aim at predicting populations in a social and geographical space under varying constraints that typically reflect a profiling of the future population through margins or combined margins. The area has received increasing attention in recent years due to an increased focus on agent-based modeling in the transportation area (Bowman and Ben-Akiva, 2001; Bradley et al., 2010). The focus on micro agents as opposed to matrices or prototypical individuals enables modelers to investigate distributional effects in the social and geographical space (Dieleman et al., 2002; Bhat and Srinivasan, 2005) and to address issues such as equity, household composition, social coherency and aging in relation to transport (Bento et al., 2005; Stead, 2001) in a more detailed fashion.

Traditionally, population synthesis models consist of several stages involving: i) the generation of a starting solution, ii) a matrix fitting stage, and iii) an allocation stage where prototypical agents are translated into micro agents and households. This approach is used in many applications (Rich, 2018; Beckman et al., 1996; Ballas et al., 2005) and combines deterministic fitting methods with micro-simulation. More recently, there has been an interest in pure simulation-based approaches (Barthelemy and Toint, 2013; Farooq et al., 2013; Harland et al., 2012), where the last two stages of the traditional approach essentially reduce to a re-sampling stage where individuals are selected from a simulated pool of individuals. The main challenge of the re-sampling stage is to generate proper sampling weights that reflect future population targets. Although this problem is not straightforward for many target variables, it can be solved by combining traditional fitting methodologies, e.g. Iterative Proportional Fitting (IPF) or simulated annealing, with quota-based sampling. The first stage of population synthesis, i.e. the generation of an appropriate starting solution, is a challenge that is relevant for all methods whether they are based on deterministic fitting or simulation.

In recent years the appetite for more detailed models has escalated and led to models that are based on yet smaller zones and have yet more refined social descriptions of individuals and households. This development has underlined the importance of population synthesis, but at the same time led to new challenges related to scalability and the ability to generate “out-of-sample” agents. These two challenges are an important and somewhat overlooked problem for MCMC-based approaches. The scalability challenge is particularly relevant for very detailed representations of the population as the samples that are typically used to start the synthesis are easily “overstretched” with the result that the sampler collapses and cannot escape the structure of the starting solution. The problem is not present for low dimensions because, in that case, the distribution space is typically densely populated by data. However, for higher dimensions, this coverage becomes very sparse, leading to the existence of isolated or loosely connected “probability density islands” which causes the sampling to be less efficient. To circumvent the problem in an MCMC context, unrealistically large samples are required. The second challenge often faced when applying MCMC approaches is related to the generation of out-of-sample agents. That is, the ability to generate agents which on the one hand share similar statistical properties as those in the original sample but are not their strict copies. However, the generation of out-of-sample agents is a highly complex problem and represents the delicate balance of replication of sample properties without overfitting. The two challenges, of scalability and “out-of-sample” generation, are closely connected as an increased dimensionality accelerates the problem of overfitting (Bishop, 2006).

This paper seeks to address precisely these two challenges by proposing a new scalable approach to population synthesis based on a Variational Autoencoder (VAE) known from machine learning. The idea is that, rather than sampling directly from a known distribution, sampling should be based on a good predictor of the joint probability distribution. The fundamental objective, therefore, is to formulate and model a distribution that overcomes the issue of scalability and overfitting. In the paper, this is tackled by using generative modeling as a means of modeling the joint distribution. Generative modeling is a subfield of statistics and machine learning which focuses on estimating the joint probability distribution of data. Traditionally, generative models based on probabilistic graphical models have suffered from scalability issues, which made them applicable either to small problems or required the introduction of simplifying assumptions. In recent years, however, deep generative models (Goodfellow et al., 2016) have opened a path toward large scale problems. These models, which combine deep neural networks and efficient scalable inference algorithms, have proven to be effective as a means of modeling high-dimensional data such as images (Radford et al., 2015) or text (Yu et al., 2017). This paper aims at extending this progress into the transportation modeling area by applying the method to the problem of population synthesis.

Main contributions of the paper are as follows. First, we connect the area of population synthesis with generative machine learning and show how a dedicated Variational Autoencoder framework (Kingma and Welling, 2013) can be tailored to the problem of population synthesis. In doing so, we take advantage of the scalability of the framework and the smoothing properties that result from encoding the joint distribution over a compressed latent space. Secondly, by dealing with potentially hundreds of mixed continuous and categorical variables, we take population synthesis to a new stage where it is eventually possible to mimic entire large-scale travel diaries, including variables that measure individual specific information and variables that measure travel preferences. Finally, we compare the proposed methodology with a conventional Gibbs sampler (Farooq et al., 2013) by using a large-scale Danish trip diary. Several things are revealed. It is shown that, whereas the Gibbs sampler generally outperforms the encoder framework when the population is spanned by few dimensions, the encoder framework outperforms the Gibbs sampler when the dimensionality increases. Also, we show that in terms of sample variability, the encoder framework renders solutions that are richer and more diverse when compared to the initial distribution, whereas the Gibbs sampler essentially replicates the agents from the original sample. It is also shown, by applying high-dimensional PCA plots, inspired from DNA sequencing (Novembre et al., 2008), that the VAE model captures the underlying data clustering structure (“data DNA”) better than the Gibbs sampler.

The rest of the paper is organized as follows. In Section 2, we briefly review existing literature and introduce the reader to generative modeling. In Section 3, we describe the methodology and present a formalization of the VAE framework. Section 4 presents the case study, which is followed by Section 5 where we present results and offer a discussion. Finally, in Section 6, a conclusion is provided.

## 2. Literature Review

### 2.1. Population synthesis

Population synthesis has been approached from mainly three methodological angles: i) reweighting, ii) matrix fitting, and iii) simulation-based approaches (Tanton, 2014). For the reweighting approach, the common method is to estimate expansion factors for a given survey such that the expanded survey reflects the target population. Reweighting typically applies non-linear optimization (Daly, 1998; Bar-Gera et al., 2009) to estimate weights and is generally not scalable to large dimensions. Matrix fitting can be seen as a generalization of any reweighting approach in the sense that it renders expansion factors that can be expressed by the ratio between the starting solution and the final matrix. Popular methods for matrix fitting include Iterative Proportion Fitting (IPF) as proposed by Deming and Stephan (1940) and maximum cross-entropy (Guo and Bhat, 2007). There is a rich literature on these methods which oversee convergence (Darroch and Ratcliff, 1972), preservation of odds-ratios (Bishop et al., 1975), model properties under convex constraints (Csiszar, 1975; Dykstra, 1985) and equivalence of cross-entropy and IPF (McDougall, 1999). Matrix fitting as well as reweighting does not produce an agent-based sample but rather a sample of prototypically weighted individuals. As a result, if the population synthesis is linked to an agent-based model, a post-simulation stage is required where individuals are drawn from the weighted sample (Rich, 2018).

The third approach to population synthesis is that of simulation. As mentioned in the introduction, most applied synthesis frameworks use a combination of deterministic approaches, such as matrix fitting and simulation, in order to facilitate the translation from matrices to individuals (e.g., Pritchard and Miller (2012); Guo and Bhat (2007)). However, pure simulation-based approaches to population synthesis involve two main stages: i) the generation of a sample pool of individuals and ii) a re-sampling stage where individuals are drawn from the sample pool. The latter stage resembles an importance sampling stage, possibly quota-based (Farrell et al., 2013), where sample weights are defined such that the final population reflect margins of future populations. Birkin and Clarke (1988) were the first to propose a simulation-based approach to population synthesis. Their methodology was to draw from conditional probability distributions of the underlying population and then gradually build a pool of individuals with a similar correlation pattern as the sample population. This is known as Gibbs sampling, which is a Markov Chain Monte Carlo (MCMC) algorithm as also considered more recently in Farooq et al. (2013). In that work, the authors also discuss the possibility of using models to approximate sampling distributions when the number of observations is small. Modeling of the joint distribution based on Bayesian networks (Sun and Erath, 2015) or Hidden Markov models (Saadi et al., 2016) has also been proposed.

In essence, the Gibbs sampler is a reversible Markov-Chain process which generates a chain of samples that will mimic the sample properties of the original sample arbitrarily close (Casella and George, 1992). Clearly, if the starting solution is poor and has missing observations, the MCMC will render an equally poor solution. A more serious problem when using MCMC models for high-dimensional distributions is related to the risk of overfitting (Justel and Pea, 1996). Generally, if the number of observations in the sample is limited, there is a limit for how many attributes the Gibbs sampler can handle. If the number of attributes becomes too large, the Gibbs sampler collapses in the sense that it cannot escape the starting solution. This issue is not new and has been recognized by several authors, including Gelman and Rubin (1992) and Hills and Smith (1992). Smith and Roberts (1993) even illustrated how the Gibbs for specific bimodal distributions may be trapped when the modes of the distribution represent disconnected islands. Although the properties of the Gibbs sampler is attractive in some low-dimensional contexts, it is not attractive in connection to population synthesis where we need to generate future populations with many attributes and such that correlation patterns and specific subsets of the population are allowed to diverge from the starting solution.

### 2.2. Generative modeling

Given observations of multiple random variables,  $X_1, \dots, X_n$ , generative modeling aims to estimate their joint probability distribution  $P(X_1, \dots, X_n)$ . This approach is different from much more popular discriminative models which learn the conditional distribution  $P(X_1|X_2, \dots, X_n)$ , where  $X_2, \dots, X_n$  are independent or input variables and  $X_1$  is a dependent or target variable to be predicted. Often, generative models are less effective in standard prediction applications when compared to their discriminative counterparts. In addition, these models are also more challenging to train because of the poor scalability. As a result, they are either restricted to small-scale problems or subject to simplified assumptions about the data generation process. This is the case for a wide range of generative models, even

very successful ones, such as Gaussian mixture models, naïve Bayes models, Hidden Markov models, Boltzmann machines and other approaches based on Probabilistic Graphical Models (Bishop, 2006).

Recently, the combination of generative models and deep learning techniques has led to efficient inference algorithms based on back-propagation (Goodfellow et al., 2016). This has made it possible to address high-dimensional data with hundreds of attributes from the perspective of generative modeling. The two most popular approaches include Variational Autoencoders (VAEs) (Kingma and Welling, 2013) and Generative Adversarial Networks (GANs) (Goodfellow et al., 2014). Both of these approaches have received a great deal of attention in the computer vision field where they are used to generate photo-realistic images (Karras et al., 2018), to address image super-resolution (Ledig et al., 2016) or compression (Gregor et al., 2016) tasks. Recently, they have also gained popularity for natural language processing (Yu et al., 2017), speech synthesis (van den Oord et al., 2016), or even in chemistry (Gmez-Bombarelli et al., 2018), astronomy (Schawinski et al., 2017) and physics (Wetzel, 2017). In the transport modeling context, deep generative models were recently applied to infer travelers’ mobility patterns from mobile phone data (Yin et al., 2018) and generate synthetic travelers’ mobility patterns in order to replicate statistical properties of real people’s behavior (Lin et al., 2017). Another application example includes generation of urbanization patterns (Albert et al., 2018), where synthetic maps of build-up areas are generated using the GAN model.

This paper aims to extend the application of this framework by generation of synthetic populations using the VAE model. Hence, while one of the main applications of VAE so far has been to generate photo-realistic fake images, this paper focuses on the generation of “pictures” of humans in the socio-demographic space, where different persons’ attributes, such as income or age, are generated instead of pixels.

### 3. Methodology

#### 3.1. Variational Autoencoder

In this subsection, we provide a high-level description of the theory behind VAE. For a more detailed discussion or mathematical rigor, we recommend readers to consider the original paper by Kingma and Welling (2013) or the tutorial by Doersch (2016).

Let us represent an agent by a vector of random variables  $X = (X_1, \dots, X_n)$  whose components can be distributed either continuously or categorically. In this case, a micro sample of the size  $N$  represents a set of observations  $\mathbf{x}_k$  ( $k = 1 : N$ ) where  $x_{ki}$  is a  $k^{\text{th}}$  observation of the  $i^{\text{th}}$  attribute.

VAE is an unsupervised generative model which is capable of learning the joint distribution  $P(X)$ . It is a latent variable model which relates the observable variables in  $X$  to a multivariate latent variable  $Z$ . The intuition behind VAE is that given  $Z$ , with some *known* distribution, e.g., multivariate Gaussian, it can be mapped using cleverly chosen nonlinear transformation such that it approximates  $P(X)$ . For instance, if  $Z$  follows a two-dimensional normal distribution, then the values of  $Z/10 + Z/\|Z\|$  will be located on a circle (see Fig. 2 in Doersch (2016)). The samples from VAE are generated via sampling the latent variable and mapping it to the observed space of  $X$ . This mapping,  $P_\phi(Z)$ , is referred to as a “decoder”, where  $\phi$  are its parameters.

A naïve way of estimating  $\phi$  is to sample values of  $Z$ , map them by the decoder and apply log-likelihood maximizing over  $\phi$  based on the observed data samples. However, this approach (which is similar to training the GAN model without a discriminator) is highly inefficient and suffers from very slow convergence. An alternative is to introduce structure to the latent space. This approach is based on the introduction of another function  $Q_\theta(X)$  with parameters  $\theta$ , referred to as the “encoder”, which maps  $X$  to  $Z$  in the first place. During the training stage, the encoder maps an input vector to the latent space, which in turn is mapped back to the observed data space by the decoder. The error is measured as the difference between the input and output vectors. This joint estimation of  $P_\phi(Z)$  and  $Q_\theta(X)$  helps the model to find an efficient representation of the data in the latent space.

To approximate any complex nonlinear mapping arbitrarily close, both decoder and encoder should have a highly flexible form. The most common choice is that of an Artificial Neural Network (ANN). In this paper, we use a fully connected multilayer ANN (described below). However, any neural network architecture suitable to the task at hand can be employed, for example, a convolutional network for data that possess a spatial structure or a recurrent one for sequential data.

In our particular case, a fully connected ANN architecture is used. It consists of multiple layers of artificial neurons. The neuron is defined in a standard way, as the weighted sum of its inputs followed by a nonlinear activation

function. Namely, the  $l^{\text{th}}$  layer of an ANN computes its output as  $\mathbf{y}_l = f(\mathbf{W}_l \mathbf{y}_{l-1} + \mathbf{b}_l)$ , where  $\mathbf{W}_l$  and  $\mathbf{b}_l$  are the weight matrix and the bias vector associated with the layer, and  $f$  is a nonlinear activation function applied element-wise to its vector argument. Further, we use the tanh function for  $f$ , however, other choices such as the rectified linear unit,  $\text{ReLU}(x) = \max(0, x)$ , can be explored. The collection of all weights and biases is denoted above as  $\phi$  and  $\theta$  for the decoder and the encoder, respectively. For numerical variables (numerical components of the vector  $X$ ), the output layer of the decoder has linear neurons, i.e. without applying  $f$ . For categorical variables, the output layer of the decoder has a soft-max form that resembles a multinomial logit formulation.

This encoder-decoder architecture used in VAE is similar to the deterministic Autoencoder model (Hinton and Salakhutdinov, 2006) which usually has a bottleneck structure with the dimensionality of  $Z$  being much less than the dimensionality of  $X$  (Fig. 1). The encoder and the decoder usually have the same form, although such that the one is a mirror of the other. For example, if the input and the latent space dimensionality are  $n$  and  $D_Z$ , respectively, and the encoder is an ANN consisting of the input layer, two hidden layers and the output layer with  $n$ - $A$ - $B$ - $D_Z$  neurons, then the decoder is also an ANN with the four layers consisting of  $D_Z$ - $B$ - $A$ - $n$  neurons (the ANN architecture is denoted as “number of neurons in layer 1”-“number of neurons in layer 2”-...). This bottleneck structure allows for learning a compressed representation of sparse data in a low-dimensional latent space.

More formally, the VAE algorithm can be summarized as follows (Fig. 2). During the training, the encoder takes a data sample  $\mathbf{x}_k$  and maps it into two parameter vectors,  $\boldsymbol{\mu}_k$  and  $\boldsymbol{\sigma}_k$ . These vectors are used to parametrize the multivariate normal distribution for generating the latent variable  $\mathbf{z}_k = \boldsymbol{\mu}_k + \boldsymbol{\sigma}_k \odot \boldsymbol{\epsilon}$ , where  $\boldsymbol{\epsilon} \sim \mathcal{N}(0, \mathbf{I})$  and  $\odot$  denotes element-wise multiplication. The fact that  $\mathbf{z}_k$  is not sampled directly is known as the reparameterization trick. This trick allows back-propagation of the reconstruction errors through the latent space back to the encoder. The back-propagation algorithm works only for continuous distributions for  $Z$  although there is ongoing research that tries to overcome this limitation (Rolfe, 2016; Maddison et al., 2016; Jang et al., 2016). Finally,  $\mathbf{z}_k$  is transformed using the decoder, and the difference between the initial  $\mathbf{x}_k$  and its reconstructed counterpart  $\hat{\mathbf{x}}_k$  is measured. The following loss function is optimized using the back-propagation algorithm with respect to the encoder and decoder parameters

$$\min_{\theta, \phi} \mathcal{L}(\theta, \phi) = \sum_k \|\mathbf{x}_k - \hat{\mathbf{x}}_k\|_{\text{num}} + \|\mathbf{x}_k - \hat{\mathbf{x}}_k\|_{\text{cat}} + \beta D_{\text{KL}}[\mathcal{N}(\boldsymbol{\mu}_k, \boldsymbol{\sigma}_k) \|\mathcal{N}(0, \mathbf{I})], \quad (1)$$

where

$$\|\mathbf{x}_k - \hat{\mathbf{x}}_k\|_{\text{num}} = \frac{1}{2} \sum_{i \in \{\text{num}\}} (x_{ik} - \hat{x}_{ik})^2 \quad (2)$$

is the mean square loss associated with the reconstruction of numerical variables, whereas

$$\|\mathbf{x}_k - \hat{\mathbf{x}}_k\|_{\text{cat}} = - \sum_{i \in \{\text{cat}\}} \sum_{j=1}^{D_i} x_{ik}^{(j)} \log \hat{x}_{ik}^{(j)} \quad (3)$$

is the cross-entropy loss associated with the reconstruction of categorical variables, taking one of the  $D_i$  possible values within a “one-hot” representation, and

$$D_{\text{KL}}[\mathcal{N}(\boldsymbol{\mu}_k, \boldsymbol{\sigma}_k) \|\mathcal{N}(0, \mathbf{I})] = -\frac{1}{2} \sum_{i=1}^{D_Z} \left( 1 + \log \sigma_{ik} - \mu_{ik}^2 - \sigma_{ik} \right) \quad (4)$$

is a regularization term represented by the Kullback-Leibler divergence between the  $D_Z$ -dimensional latent variable distribution parametrized by the encoder output (mean  $\boldsymbol{\mu}_k$  and standard deviation  $\boldsymbol{\sigma}_k$ ) and the Gaussian prior  $\mathcal{N}(0, \mathbf{I})$ . This term enforces the learned distribution of the latent variable to have the desired form. It makes sampling of the latent space possible in contrast to the deterministic Autoencoder model where the associated latent space lacks any probabilistic meaning. Here,  $\beta$  is a hyper-parameter representing a weighting coefficient between the reconstruction losses and the regularization strength (Higgins et al., 2017).

When the model has been trained, new samples can be generated by sampling of the latent variable from the prior distribution  $\mathcal{N}(0, \mathbf{I})$  and transforming it through the decoder to the data space. In this case, exploring new regions of the latent space will result in new out-of-sample agents that differ from those from the original data used for training. For instance, sampling values across the line connecting two points in the latent space will result in the generation of

agents characterized by a mixture of attributes of the corresponding “edge” agents. Moreover, the dimensions of the latent variable  $Z$  can be interpretable. This behavior is more prominent for image data, when varying one of the latent dimensions with the others being fixed can reveal that, for instance, it might be responsible for the object’s position, color or size. However, these properties are not so obvious in the case of non-visual data such as those considered in the present work.

The VAE model can also address anomaly detection and data imputation problems. For example, the probability of an agent to be present in the data can be estimated in the latent space using the agent’s mapping via the encoder. Missing values for attributes of an agent can be imputed by minimizing the distance between the known attributes of the agent and its reconstructed counterpart by using gradient descent in the latent space.

### 3.2. Gibbs sampling

MCMC methods are a set of popular tools to facilitate sampling from complex distributions. They are widely used in many domains including computer science, machine learning, physics, and finance. Gibbs sampling is one of many MCMC algorithms that works by sampling from the available conditional distributions  $p(x_i|x_{-i}) \equiv p(x_i|x_1, \dots, x_{i-1}, x_{i+1}, \dots, x_n)$ . The process is equivalent to a sampling scheme from the joint distribution such that  $p(x_i|x_{-i}) = p(x_i, x_{-i})/p(x_{-i}) \propto p(x_i, x_{-i})$ . The standard algorithm includes two fundamental steps. First, a starting point  $\mathbf{x}^{(0)}$  is defined. In the second step, the value of each component  $x_i^{(0)}$  is updated according to  $p(x_i|x_1^{(1)}, \dots, x_{i-1}^{(1)}, x_{i+1}^{(0)}, \dots, x_n^{(0)})$ , until all components are updated and a new sample  $\mathbf{x}^{(1)}$  is obtained. Typically, to reach a stationary state, a “warm-up” stage is carried out. This stage is accomplished by eliminating the first  $N_{\text{wu}}$  samples from the sample pool. Also, to avoid correlation between samples, each consequent  $N_{\text{th}}$  sample is kept while samples in between are eliminated.

It is important to stress that all MCMC algorithms are designed to *sample* from a complex distribution rather than *approximate* it. Therefore, it is a crucial problem how the underlying sampling distributions are prepared in the first place.

In the simplest case, the conditional probabilities required for the Gibbs sampler can be provided in the form of multidimensional frequency tables. These tables can be estimated either from aggregated statistics or using empirical counts from an available micro sample. In this case, MCMC sampling will simply revisit cells of the frequency table and generate agents corresponding to each cell. Categorical attributes of the agents used to estimate the conditional probabilities will be exactly reproduced. Numerical attributes will contain sampling noise proportional to the size of these cells since the sampling does not make any distinction between the values within a cell, so any numerical value can be uniformly chosen. Obviously, in this case, MCMC sampling does not bring any additional benefits when the micro sample is available. It effectively simplifies to uniform expansion of the pool of initial agents, reproducing the underlying population to perfection. For the case study, we illustrate this problem by approximating the conditionals as empirical counts and comparing generated samples with the original micro sample.

It is also possible to consider different levels of aggregation for the conditional probabilities, from full conditionals, when all  $p(x_i|x_{-i})$  are known, to marginals, when only  $p(x_i)$  are available. The latter corresponds to the edge case of the “collapsed Gibbs sampler” (Liu, 1994) where all other variables are marginalized. The collapsed Gibbs sampler, which uses partial conditionals  $p(x_i|x_{-i-j, \dots})$ , is often used to reduce computational costs and accelerate sampling. It can also mitigate the problem of the sampler being trapped in a local minimum. This situation arises when the distribution is multimodal and the modes are connected with low probability domains or are completely disconnected. This problem might also be addressed by generating several chains from different starting points. However, this approach quickly becomes infeasible in higher dimensions, where the volume of the space to cover grows exponentially with the number of the dimensions involved. The benefits of the collapsed Gibbs sampler come at the cost of neglecting statistical dependencies between the marginalized and remaining variables. Clearly, if only marginals  $p(x_i)$  are used, the corresponding samples will have the lowest quality.

Nevertheless, the MCMC approach can be beneficial when there is no access to the data used to calculate the frequency tables or there are other partial views of the joint distribution (Farooq et al., 2013). It is also useful when the sampling distributions are non-trivially approximated in the first place, for example, using probabilistic graphical models (Sun and Erath, 2015; Saadi et al., 2016) or parametric models that make explicit assumptions about the data generation process (Farooq et al., 2013). These approaches are particularly suitable when the micro sample is very small and can facilitate the generation of out-of-sample agents.

## 4. Case study

We consider the problem of generating a synthetic population with both numerical (e.g. income) and categorical (e.g. gender or education level) attributes on the basis of a large-scale trip diary in Denmark. More specifically, we use the Danish National Travel Survey (TU) data<sup>1</sup>, which is known to be one of the largest coherent trip diaries worldwide. It contains 24-hour trip diaries for more than 330,000 Danish residents and provides detailed information for approximately 1 million trips in the period from 1992 to present. In this paper, we use the TU sample from 2006–2017, representing more than 146,000 unique respondents.

As the data contain both numerical and categorical variables, we consider two approaches: i) discretization of the numerical variables by converting them into categorical variables using the number of bins defined in the third column in Table 1 and ii) working directly with the mixture of both. While the latter makes less assumptions about the variables, the former can approximate the continuous case depending on the resolution of the discretization bins. We use a “one-hot” encoding of the categorical variables. For example, if a discretized number of persons in the household can take one of the categorical values “1”, “2”, “3”, “4” or “5+”, then the household with 2 persons will correspond to the vector (0, 1, 0, 0, 0). Hence, the dimensionality of the problem is directly proportional to the number of possible categories. We selected three subsets of individual attributes for each person defined in Table 1:

1. *Basic* attributes are similar to the test case used in Farooq et al. (2013) and contain 2 numerical (person’s age and number of people in the household) and 2 categorical (person’s gender and educational attainment) variables. The resulting distribution is however 14-dimensional (and 27-dimensional when the numerical variables are discretized).
2. *Socio* attributes contain more detailed socio-demographic information and comprise 8 numerical and 13 categorical variables, where the resulting distribution is 68-dimensional (121-dimensional when the numerical variables are discretized).
3. *Extended* attributes additionally include data related to work and travel behavior and contain all 47 variables, 21 numerical and 26 categorical, making the resulting distribution 230-dimensional (357-dimensional when the numerical variables are discretized).

The high dimensionality of the problem makes any use of the IPF algorithm impossible as the number of the corresponding matrix cells grows exponentially with the number of dimensions. For example, considering  $m$  binary variables requires fitting of  $2^m$  cells which quickly makes the algorithm impractical for large  $m$ . Furthermore, we show that the standard Gibbs sampling algorithm becomes trapped in the local minimum around its starting point in such high dimensions that one needs to resort to scalable deep learning solutions. The three subsets of individual attributes are used to create three separate datasets for the comparison of the methods in the following section.

## 5. Results and Discussion

### 5.1. Model specification and validation

To compare performance of the methods, we use a 20% micro sample (MS) of the data for training (held-in data) while the remaining data, also referred to as the “true” population, are used for validation purposes (held-out data). In the Gibbs sampler context, the training data are used to calculate the underlying sampling distributions (conditionals or marginals) as frequency tables. The three subsets of attributes (Basic, Socio and Extended) are used to run three separate experiments. A pool of 100,000 agents is synthesized using each method, i.e. VAE, Gibbs sampler for full conditionals (Gibbs-cond), and Gibbs sampler for marginals (Gibbs-marg). For both Gibbs samplers, the first  $N_{\text{wu}} = 20000$  samples are discarded and each successive  $N_{\text{th}} = 20$  sample is kept, requiring 2,020,000 iterations to generate the pools. The methods are compared by comparing the statistical properties of the synthesized samples with the properties of the held-out data. The code is available at <https://github.com/stasmix/popsynth>.

To optimize the hyper-parameters of VAE, the training set for VAE is further subdivided into an actual training set, which is used to fit VAE parameters (weights and biases of the encoder and decoder), and a development set that is used to compare performance of the models with the different architectures and values of the hyper-parameters. The

---

<sup>1</sup><http://www.modelcenter.transport.dtu.dk/english/tvu>

hyper-parameters are optimized using grid search. For the encoder, we explore a fully connected ANN architecture consisting of 1, 2 or 3 hidden layers with 25, 50, 100; 50-25, 100-50; or 100-50-25 neurons, respectively. The decoder has the mirrored architecture of the encoder. The dimensionality of the latent space,  $D_Z$ , takes one of the following values: 5, 10, 25. For  $\beta$ , we use the values of 0.01, 0.05, 0.1, 0.5, 1.0, 10, 100. For the training, the RMSprop algorithm with the learning rate of 0.01 and  $\rho = 0.9$  is used, the size of a mini-batch is 64 and the number of epochs is 100. The numerical data are normalized before training to have zero mean and unit standard deviation.

To estimate how well synthetic agents are able to reproduce the statistical properties of the true population, we compare corresponding synthetic  $\hat{\pi}$  and true  $\pi$  distributions. The distributions are represented as multidimensional histograms of the two samples, where numerical variables are discretized during the comparison as mentioned earlier. As in previous works, three standard metrics are calculated: Standardized root mean squared error (SRMSE),

$$\text{SRMSE}(\hat{\pi}, \pi) = \frac{\text{RMSE}(\hat{\pi}, \pi)}{\bar{\pi}} = \frac{\sqrt{\sum_i \cdots \sum_j (\hat{\pi}_{i\dots j} - \pi_{i\dots j})^2 / N_b}}{\sum_i \cdots \sum_j \pi_{i\dots j} / N_b}, \quad (5)$$

Pearson correlation coefficient (Corr) and coefficient of determination ( $R^2$ ). The last two are defined in a standard way for the same bin frequencies  $\pi_{i\dots j}$  and  $\hat{\pi}_{i\dots j}$  and the total number of bins  $N_b$ .

It is worth noting that the comparison of high-dimensional distributions (and generative models in general) represents an ongoing research challenge (Theis et al., 2015). The main problem with the kernel density estimation in high dimensions is that even a large number of samples generally do not allow estimating the true log-likelihood of the model due to the curse of dimensionality (the amount of data to uniformly fill a hypercube grows exponentially with the dimensionality of the hypercube). Therefore, we restrict ourselves to the comparison of low-dimensional projections of the distributions with respect to the Basic attributes only. For the remaining variables, we resort to visual inspection of their margins.

Manual inspection of individual synthetic agents is more challenging than for the standard generative model applications such as image, sound or text. An alternative approach, which is inspired by the mapping of DNA sequences (Novembre et al., 2008), is to perform a multi-dimensional Principal Component Analysis (PCA) to visualize the synthesized agents in 2D. PCA is a method to find orthogonal decomposition of the data where each vector corresponds to the direction of the highest possible variance. In machine learning, it is widely used for visualization of high-dimensional data which also helps to reveal clusters in the data. We use projections of the synthesized agents onto different principal components (eigenvectors) to visually inspect clustering of the synthetic population and compare it to the original micro sample.

To investigate the diversity of the generated samples, i.e. the ability of a model to generate out-of-sample agents instead of replicating the training data, we introduce the following procedure. For each sample generated by the model,  $\mathbf{x}_i^{\text{gen}}$ , we calculate its distance to all the samples used for training,  $\mathbf{x}_j^{\text{train}}$ , as  $\text{RMSE}(\mathbf{x}_i^{\text{gen}}, \mathbf{x}_j^{\text{train}})$  and find the nearest sample. Then, we calculate mean,  $\mu_{\text{NS}}$ , and standard deviation,  $\sigma_{\text{NS}}$ , of these nearest sample distances over all the generated samples. Thus, for the model which perfectly replicates the training data,  $\mu_{\text{NS}} = 0$  and  $\sigma_{\text{NS}} = 0$ . For the Gibbs-marg sampler that uses only information from marginals and therefore does not capture statistical dependencies between the variables, these validation parameters tend to attain high values. However, it is difficult to interpret their values other than zero.

## 5.2. Comparison of methods

Table 2 summarizes the main results. As the first baseline, we use the Gibbs-marg sampler which samples the marginal distribution of each variable, generating its value independently from the rest of the variables. The population generated by the Gibbs-marg sampler perfectly reproduces the marginals of the true population, however it has a very high error (SRMSE = 1.740; Fig. 3, last row) due to neglecting statistical dependencies between the attributes. As the second baseline, we show the micro sample used for training itself. The micro-sample (MS) naturally represents the best possible approximation to the true population given that it is the only information available about the true population. Its uniform expansion (re-sampling with replacement) produces the best results in terms of performance metrics (SRMSE = 0.181; Fig. 3, last row). However, this approach is clearly incapable of generating new out-of-sample individuals (in Table 2, the diversity measures  $\mu_{\text{NS}} = 0.002$  and  $\sigma_{\text{NS}} = 0.048$  for the MS are calculated for the held-out data in contrast to the rest of the models).



The Gibbs-cond sampler outperforms VAE only in the low-dimensional case when the Basic attributes are considered (Fig. 3, first row). Its performance (SRMSE = 0.196 for discretized numerical variables and SRMSE = 0.201 for non-discretized) is close to the performance of the MS itself. The performance of VAE is almost three times worse (SRMSE = 0.481 and 0.676, respectively). However, the agents generated by the Gibbs-cond sampler are essentially a replication of the training data for the case where the numerical variables are converted to categorical since corresponding  $\mu_{NS}$  and  $\sigma_{NS}$  are exactly equal to zero. In the case where the mixture of both categorical and numerical variables is used, the Gibbs-cond sampler introduces noise that depends on the size of the bins used to estimate the conditional probabilities as mentioned before.

For the two remaining high-dimensional cases, VAE significantly outperforms the Gibbs sampler. When the attributes from the Socio set are considered, the Gibbs-cond sampler clearly becomes trapped in a local minimum around the starting point (Fig. 3, second row). For the Extended attributes, the Gibbs-cond sampler cannot even escape the starting point (Fig. 3, third row). At the same time, the performance of VAE remains acceptable: Its SMRSE increases from 0.481 to 0.693 for the Socio attributes and to 0.959 for the Extended attributes when numerical variables are discretized. For the mixture of both, the error increases to 0.846 and 1.184, respectively. Nevertheless, these values are still below the error of the Gibbs-marg sampler.

Despite a relatively high SRMSE, the marginal distributions for the pool of agents generated using VAE indicate a very good correspondence with the held-out data. For instance, Fig. 4 shows marginals for eight selected attributes from the Extended set. Although there are inconsistencies for the low probability values of some attributes (e.g. discretized GISdistHW in Fig. 4a or WorkHoursPw in Fig. 4b), the values that have high probability are captured correctly.

Increasing the number of training epochs from 100 to 200 for the VAE trained on the Extended set slightly reduces SMRSE of the best performing model from 0.959 to 0.912 for discretized numerical variables and from 1.184 to 1.053 for non-discretized ones. This behavior suggests that the training stopped before reaching a minimum of the loss function (Eq. (1)). Early stopping is known to be one of the regularization techniques used to prevent overfitting. However, the most important feature of VAE that helps to avoid this problem is its bottleneck structure. Indeed, the model is able to compress the data from initially sparse 357-dimensional space into the 25-dimensional latent space representation (Table 3). The Basic and Socio attributes are compressed from 27 to 5 dimensions and from 121 to 10 dimensions respectively. Finally, all  $\mu_{NS}$  and  $\sigma_{NS}$  are non-zero for all the VAE models. Therefore, we can expect that VAE does in fact generalize as opposed to simply memorizing the training data.

As mentioned before, it is difficult to manually inspect the agents generated by VAE and to conclude whether they represent plausible individuals or not. One of the possible ways is to test the synthetic population for logical inconsistencies using a predefined set of rules. For instance, the inconsistencies could be classified as children with university degrees or unemployed individuals with non-zero working hours. As an example, the same subset of marginal distributions from Fig. 4 is plotted for the individuals who are under 20 years old in Fig. 5. These distributions are quite different from the whole population, especially for personal income (IncRespondent), educational attainment (RespEdulevel), main occupation (RespMainOccup) and possession of a driving license (ResphasDrivlic). The VAE model correctly reproduces the observed pattern apart from some low probability domains.

While it is feasible to inspect such pairwise correlations based on handcrafted rules for a small set of attributes, this approach becomes impracticable for a large number of attributes, especially taking into account high-order correlations (e.g. when an employed person who lives close to the place of occupation has long commuting time). To address this issue, we visualize the high-order clustering structure of the data using PCA. The PCA analysis of the agents generated by VAE (Fig. 6) for the Basic attributes shows that they have a clustering structure similar to that of the training data. However, for the agents generated by the Gibbs-cond sampler, the second principal component shows less agreement with the training data although the overall error of the sampler is much lower.

When the mixture of both numerical and categorical variables is used, VAE shows slightly worse performance compared to the case when the numerical variables are converted to categorical. This might be due to the coarse grid of hyper-parameters and the limited number of ANN architectures explored. Additionally, separate log-likelihood weighting factors of the numerical and categorical terms in the loss function (Eq. (1)) can be introduced. However, this approach quickly becomes computationally expensive as the dimensionality of the optimization grid grows exponentially with the number of hyper-parameters involved. Nevertheless, as mentioned before, it is possible to avoid this problem by converting numerical variables to categorical using a sufficiently high resolution of the discretization bins.

## 6. Conclusions and future work

This paper presents a scalable approach to the problem of generating large sample pools of agents for use in micro simulations of transport systems. The approach is based on deep generative modeling framework and is capable of generating synthetic populations with potentially hundreds of mixed continuous and categorical attributes. This opens a path toward modeling of a population with an unprecedented level of detail, including smaller zones, personal details and travel preferences.

The proposed approach is based on unsupervised learning of the joint distribution of the data using a Variational Autoencoder (VAE) model. The model uses a deep artificial neural network that transforms the initially sparse data into a compressed latent space representation. This compressed representation allows for efficient sampling as compared to approaches that rely on approximating the joint distribution in the observed data space. A study case is presented which involves the synthesis of agents from a large Danish travel diary, where around 29,000 records about its participants are used as held-in data and around 117,000 records are used as held-out data. It is shown how the MCMC-based Gibbs sampler already becomes trapped in local minima when 21 variables (13 categorical and 8 numerical) are used, while the VAE model still shows acceptable performance for the generation of agents with 47 attributes (26 categorical and 21 numerical). Moreover, VAE allows for growing “out-of-sample” agents which are different from the agents present in the training data but preserve the same statistical properties and dependencies as in the original data. This is contrary to the Gibbs sampler that tends to replicate the agents from the original sample over and over again when the underlying conditional distributions are approximated as multidimensional frequency tables.

This ability of generative models to generate out-of-sample agents can be used to explore a richer set of modeling scenarios. It also addresses data privacy issues since these agents do not directly correspond to real people anymore. This feature can facilitate creation of publicly open datasets by fitting generative models to the data containing private information. These synthetic datasets can be used, for example, to test models that were initially tailored for specific cases on a wider range of scenarios.

### 6.1. Future work

In this paper, the most basic VAE architecture is considered. The most straightforward extension of the proposed model is the conditional VAE (Sohn et al., 2015), which estimates probability distributions conditional on other variables. For instance, it can be used to address the job formation problem where the job distribution is conditional on the underlying population. Numerous other variations of VAEs can also be explored, such as discrete latent space VAE (Jang et al., 2016), Wasserstein VAE (Tolstikhin et al., 2017) or Ladder VAE (Sønderby et al., 2016) to name a few. The VAE model can also incorporate a recurrent neural network architecture to generate sequential data, such as fine-grained daily activity chains including time, locations, transportation modes and purpose. Finally, other deep generative models can be explored. For example, generative adversarial networks can potentially produce agents with less logical inconsistencies; they are, however, much more difficult to train in practice.

In the current work, only the first stage of simulation-based approaches related to growing pools of micro agents is addressed. The next important stage involves re-sampling, where individuals are selected from the simulated pool in such a way that the resulting population is aligned with imposed properties of future populations. In this way, changes in income and age composition can be reflected. Another challenge that can be addressed at the re-sampling stage is the explicit elimination of illogical or inconsistently generated agents. This may involve the elimination of children with full-time work or high income. For the generation of complete trip diaries, this challenge becomes non-trivial, because the spatio-temporal ordering of the activities needs to be preserved.

## Acknowledgements

The research leading to these results has received funding from the European Union’s Horizon 2020 research and innovation programme under the Marie Skłodowska-Curie grant agreement No. 713683 (COFUNDfellowsDTU), and from the European Union’s Horizon 2020 research and innovation programme under the Marie Skłodowska-Curie Individual Fellowship H2020-MSCA-IF-2016, ID number 745673.

## References

- Albert, A., Strano, E., Kaur, J., Gonzalez, M. C., 2018. Modeling urbanization patterns with generative adversarial networks. CoRR abs/1801.02710.  
URL <http://arxiv.org/abs/1801.02710>
- Ballas, D., Clarke, G., Dorling, D., Eyre, H., Thomas, B., Rossiter, D., 2005. Simbritain: a spatial microsimulation approach to population dynamics. *Population, Space and Place* 11 (1), 13–34.  
URL <https://onlinelibrary.wiley.com/doi/abs/10.1002/psp.351>
- Bar-Gera, H., Konduri, K. C., Sana, B., Ye, X., Pendyala, R. M., 2009. Estimating survey weights with multiple constraints using entropy optimization methods. *Tech. rep.*
- Barthelemy, J., Toint, P. L., 2013. Synthetic population generation without a sample. *Transportation Science* 47 (2), 266–279.  
URL <https://pubsonline.informs.org/doi/abs/10.1287/trsc.1120.0408>
- Beckman, R. J., Baggerly, K. A., McKay, M. D., 1996. Creating synthetic baseline populations. *Transportation Research Part A: Policy and Practice* 30 (6), 415–429.  
URL <http://www.sciencedirect.com/science/article/pii/S0965856496000043>
- Bento, A. M., Cropper, M. L., Mobarak, A. M., Vinha, K., 2005. The effects of urban spatial structure on travel demand in the United States. *The Review of Economics and Statistics* 87 (3), 466–478.  
URL <http://www.jstor.org/stable/40042942>
- Bhat, C. R., Srinivasan, S., 2005. A multidimensional mixed ordered-response model for analyzing weekend activity participation. *Transportation Research Part B: Methodological* 39 (3), 255–278.  
URL <http://www.sciencedirect.com/science/article/pii/S0191261504000475>
- Birkin, M., Clarke, M., 1988. Synthesisa synthetic spatial information system for urban and regional analysis: Methods and examples. *Environment and Planning A: Economy and Space* 20 (12), 1645–1671.  
URL <https://doi.org/10.1068/a201645>
- Bishop, C. M., 2006. *Pattern Recognition and Machine Learning (Information Science and Statistics)*. Springer-Verlag, Berlin, Heidelberg.
- Bishop, Y., Fienberg, S., Holland, P., 1975. *Discrete Multivariate Analysis: Theory and Practice*. Massachusetts Institute of Technology Press.  
URL <https://books.google.dk/books?id=apQDnwEACAAJ>
- Bowman, J., Ben-Akiva, M., 2001. Activity-based disaggregate travel demand model system with activity schedules. *Transportation Research Part A: Policy and Practice* 35 (1), 1–28.  
URL <http://www.sciencedirect.com/science/article/pii/S0965856499000439>
- Bradley, M., Bowman, J. L., Griesenbeck, B., 2010. Sacsim: An applied activity-based model system with fine-level spatial and temporal resolution. *Journal of Choice Modelling* 3 (1), 5–31.  
URL <http://www.sciencedirect.com/science/article/pii/S1755534513700277>
- Casella, G., George, E. I., 1992. Explaining the Gibbs sampler. *The American Statistician* 46 (3), 167–174.  
URL <https://www.tandfonline.com/doi/abs/10.1080/00031305.1992.10475878>
- Csiszar, I., 1975.  $i$ -divergence geometry of probability distributions and minimization problems. *Ann. Probab.* 3 (1), 146–158.  
URL <https://doi.org/10.1214/aop/1176996454>
- Daly, A., 1998. Prototypical sample enumeration as a basis for forecasting with disaggregate models. In: *Proceedings of the European Transport Annual Meeting*. PTRC, London. Vol. P423. pp. 225–236.
- Darroch, J. N., Ratcliff, D., 1972. Generalized iterative scaling for log-linear models. *Ann. Math. Statist.* 43 (5), 1470–1480.  
URL <https://doi.org/10.1214/aoms/1177692379>
- Deming, W. E., Stephan, F. F., 1940. On a least squares adjustment of a sampled frequency table when the expected marginal totals are known. *Ann. Math. Statist.* 11 (4), 427–444.  
URL <https://doi.org/10.1214/aoms/1177731829>
- Dieleman, F. M., Dijst, M., Burghouwt, G., 2002. Urban form and travel behaviour: Micro-level household attributes and residential context. *Urban Studies* 39 (3), 507–527.  
URL <https://doi.org/10.1080/00420980220112801>
- Doersch, C., Jun, 2016. Tutorial on Variational Autoencoders. arXiv preprint arXiv:1606.05908.
- Dykstra, R. L., 1985. An iterative procedure for obtaining  $i$ -projections onto the intersection of convex sets. *The Annals of Probability* 13 (3), 975–984.  
URL <http://www.jstor.org/stable/2243723>
- Farooq, B., Bierlaire, M., Hurtubia, R., Fltlerd, G., 2013. Simulation based population synthesis. *Transportation Research Part B: Methodological* 58, 243–263.  
URL <http://www.sciencedirect.com/science/article/pii/S0191261513001720>
- Farrell, N., Morrissey, K., O’Donoghue, C., 2013. *Creating a Spatial Microsimulation Model of the Irish Local Economy*. Springer Netherlands, Dordrecht, pp. 105–125.  
URL [https://doi.org/10.1007/978-94-007-4623-7\\_7](https://doi.org/10.1007/978-94-007-4623-7_7)
- Gelman, A., Rubin, D. B., 1992. Inference from iterative simulation using multiple sequences. *Statist. Sci.* 7 (4), 457–472.  
URL <https://doi.org/10.1214/ss/1177011136>
- Goodfellow, I., Bengio, Y., Courville, A., 2016. *Deep Learning*. MIT Press, <http://www.deeplearningbook.org>.
- Goodfellow, I., Pouget-Abadie, J., Mirza, M., Xu, B., Warde-Farley, D., Ozair, S., Courville, A., Bengio, Y., 2014. Generative adversarial nets. In: *Advances in neural information processing systems*. pp. 2672–2680.
- Gregor, K., Besse, F., Jimenez Rezende, D., Danihelka, I., Wierstra, D., 2016. Towards conceptual compression. In: Lee, D. D., Sugiyama, M., Luxburg, U. V., Guyon, I., Garnett, R. (Eds.), *Advances in Neural Information Processing Systems 29*. Curran Associates, Inc., pp. 3549–3557.  
URL <http://papers.nips.cc/paper/6542-towards-conceptual-compression.pdf>

- Guo, J., Bhat, C., 2007. Population synthesis for microsimulating travel behavior. *Transportation Research Record: Journal of the Transportation Research Board* 2014, 92–101.  
URL <https://doi.org/10.3141/2014-12>
- Gmez-Bombarelli, R., Wei, J. N., Duvenaud, D., Hernandez-Lobato, J. M., Sanchez-Lengeling, B., Sheberla, D., Aguilera-Iparraguirre, J., Hirzel, T. D., Adams, R. P., Aspuru-Guzik, A., 2018. Automatic chemical design using a data-driven continuous representation of molecules. *ACS Central Science* 4 (2), 268–276.  
URL <https://doi.org/10.1021/acscentsci.7b00572>
- Harland, K., Heppenstall, A., Smith, D., Birkin, M., 2012. Creating realistic synthetic populations at varying spatial scales: A comparative critique of population synthesis techniques. *Journal of Artificial Societies and Social Simulation* 15 (1), 1.  
URL <http://jasss.soc.surrey.ac.uk/15/1/1.html>
- Higgins, I., Matthey, L., Pal, A., Burgess, C., Glorot, X., Botvinick, M., Mohamed, S., Lerchner, A., 2017. beta-vae: Learning basic visual concepts with a constrained variational framework. *International Conference on Learning Representations*.  
URL <https://openreview.net/forum?id=Sy2fzU9gl>
- Hills, S. E., Smith, A. F., 1992. Parameterization issues in Bayesian inference. *Bayesian statistics* 4, 227–246.
- Hinton, G. E., Salakhutdinov, R. R., 2006. Reducing the dimensionality of data with neural networks. *Science* 313 (5786), 504–507.  
URL <http://science.sciencemag.org/content/313/5786/504>
- Jang, E., Gu, S., Poole, B., 2016. Categorical reparameterization with gumbel-softmax. *arXiv preprint arXiv:1611.01144*.
- Justel, A., Pea, D., 1996. Gibbs sampling will fail in outlier problems with strong masking. *Journal of Computational and Graphical Statistics* 5 (2), 176–189.  
URL <https://amstat.tandfonline.com/doi/abs/10.1080/10618600.1996.10474703>
- Karras, T., Aila, T., Laine, S., Lehtinen, J., 2018. Progressive growing of GANs for improved quality, stability, and variation. In: *International Conference on Learning Representations*.  
URL <https://openreview.net/forum?id=Hk99zCeAb>
- Kingma, D. P., Welling, M., 2013. Auto-encoding variational bayes. *arXiv preprint arXiv:1312.6114*.
- Ledig, C., Theis, L., Huszar, F., Caballero, J., Aitken, A. P., Tejani, A., Totz, J., Wang, Z., Shi, W., 2016. Photo-realistic single image super-resolution using a generative adversarial network. *CoRR abs/1609.04802*.  
URL <http://arxiv.org/abs/1609.04802>
- Lin, Z., Yin, M., Feygin, S., Sheehan, M., Paiement, J.-F., Pozdnoukhov, A., 2017. Deep generative models of urban mobility.
- Liu, J. S., 1994. The collapsed Gibbs sampler in Bayesian computations with applications to a gene regulation problem. *Journal of the American Statistical Association* 89 (427), 958–966.  
URL <https://doi.org/10.1080/01621459.1994.10476829>
- Maddison, C. J., Mnih, A., Teh, Y. W., 2016. The concrete distribution: A continuous relaxation of discrete random variables. *arXiv preprint arXiv:1611.00712*.
- McDougall, R., 1999. Entropy Theory and RAS are Friends. *Tech. rep.*
- Novembre, J., Johnson, T., Bryc, K., Kutalik, Z., Boyko, A. R., Auton, A., Indap, A., King, K. S., Bergmann, S., Nelson, M. R., Stephens, M., Bustamante, C. D., 08 2008. Genes mirror geography within europe. *Nature* 456, 98–101.  
URL <http://dx.doi.org/10.1038/nature07331>
- Pritchard, D. R., Miller, E. J., May 2012. Advances in population synthesis: fitting many attributes per agent and fitting to household and person margins simultaneously. *Transportation* 39 (3), 685–704.  
URL <https://doi.org/10.1007/s11116-011-9367-4>
- Radford, A., Metz, L., Chintala, S., 2015. Unsupervised representation learning with deep convolutional generative adversarial networks. *arXiv preprint arXiv:1511.06434*.
- Rich, J., 2018. Large-scale spatial population synthesis for Denmark. *Submitted to European Transport Research Review*.
- Rolfe, J. T., 2016. Discrete variational autoencoders. *arXiv preprint arXiv:1609.02200*.
- Saadi, I., Mustafa, A., Teller, J., Farooq, B., Cools, M., 2016. Hidden markov model-based population synthesis. *Transportation Research Part B: Methodological* 90, 1 – 21.  
URL <http://www.sciencedirect.com/science/article/pii/S0191261515300904>
- Schawinski, K., Zhang, C., Zhang, H., Fowler, L., Santhanam, G. K., 2017. Generative adversarial networks recover features in astrophysical images of galaxies beyond the deconvolution limit. *Monthly Notices of the Royal Astronomical Society: Letters* 467 (1), L110–L114.  
URL <http://dx.doi.org/10.1093/mnrasl/slx008>
- Smith, A. F., Roberts, G. O., 1993. Bayesian computation via the Gibbs sampler and related Markov chain Monte Carlo methods. *Journal of the Royal Statistical Society. Series B (Methodological)*, 3–23.
- Sohn, K., Lee, H., Yan, X., 2015. Learning structured output representation using deep conditional generative models. In: Cortes, C., Lawrence, N. D., Lee, D. D., Sugiyama, M., Garnett, R. (Eds.), *Advances in Neural Information Processing Systems* 28. Curran Associates, Inc., pp. 3483–3491.  
URL <http://papers.nips.cc/paper/5775-learning-structured-output-representation-using-deep-conditional-generative-models.pdf>
- Sønderby, C. K., Raiko, T., Maaløe, L., Sønderby, S. K., Winther, O., 2016. Ladder variational autoencoders. In: Lee, D. D., Sugiyama, M., Luxburg, U. V., Guyon, I., Garnett, R. (Eds.), *Advances in Neural Information Processing Systems* 29. Curran Associates, Inc., pp. 3738–3746.  
URL <http://papers.nips.cc/paper/6275-ladder-variational-autoencoders.pdf>
- Stead, D., 2001. Relationships between land use, socioeconomic factors, and travel patterns in britain. *Environment and Planning B: Planning and Design* 28 (4), 499–528.  
URL <https://doi.org/10.1068/b2677>
- Sun, L., Erath, A., 2015. A bayesian network approach for population synthesis. *Transportation Research Part C: Emerging Technologies* 61, 49 – 62.

- URL <http://www.sciencedirect.com/science/article/pii/S0968090X15003599>
- Tanton, R., 2014. A Review of Spatial Microsimulation Methods. *International Journal of Microsimulation* 7 (1), 4–25.  
URL <https://ideas.repec.org/a/ijm/journal/v7y2014i1p4-25.html>
- Theis, L., Oord, A. v. d., Bethge, M., 2015. A note on the evaluation of generative models. arXiv preprint arXiv:1511.01844.
- Tolstikhin, I., Bousquet, O., Gelly, S., Schoelkopf, B., 2017. Wasserstein auto-encoders. arXiv preprint arXiv:1711.01558.
- van den Oord, A., Dieleman, S., Zen, H., Simonyan, K., Vinyals, O., Graves, A., Kalchbrenner, N., Senior, A., Kavukcuoglu, K., 2016. Wavenet: A generative model for raw audio.  
URL <https://arxiv.org/abs/1609.03499>
- Wetzel, S. J., Aug 2017. Unsupervised learning of phase transitions: From principal component analysis to variational autoencoders. *Phys. Rev. E* 96, 022140.  
URL <https://link.aps.org/doi/10.1103/PhysRevE.96.022140>
- Yin, M., Sheehan, M., Feygin, S., Paiement, J. F., Pozdnoukhov, A., June 2018. A generative model of urban activities from cellular data. *IEEE Transactions on Intelligent Transportation Systems* 19 (6), 1682–1696.
- Yu, L., Zhang, W., Wang, J., Yu, Y., 2017. Seqgan: Sequence generative adversarial nets with policy gradient. *AAAI Conference on Artificial Intelligence*.  
URL <https://www.aaai.org/ocs/index.php/AAAI/AAAI17/paper/view/14344>

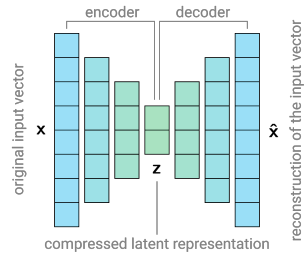


Figure 1: Schematic depiction of deterministic Autoencoder. Here, the decoder is a fully connected artificial neural network consisting of the input layer, two hidden layers and the latent representation layer. The decoder has the inverse architecture. The Autoencoder model learns to compress the input vector  $\mathbf{x}$  with 8 dimensions into the latent representation  $\mathbf{z}$  with 2 dimensions and reconstruct it back to the data space.

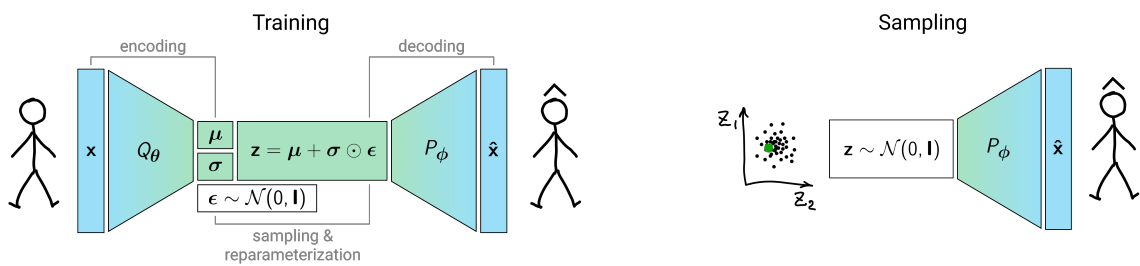


Figure 2: Schematic depiction of Variational Autoencoder. VAE learns to map (“decode”) the distribution of latent variable  $Z$  (for example, multivariate Gaussian) into the data space to approximate  $P(X)$ . This process is facilitated by learning the latent space representation (“encoding”) of the data during the training.

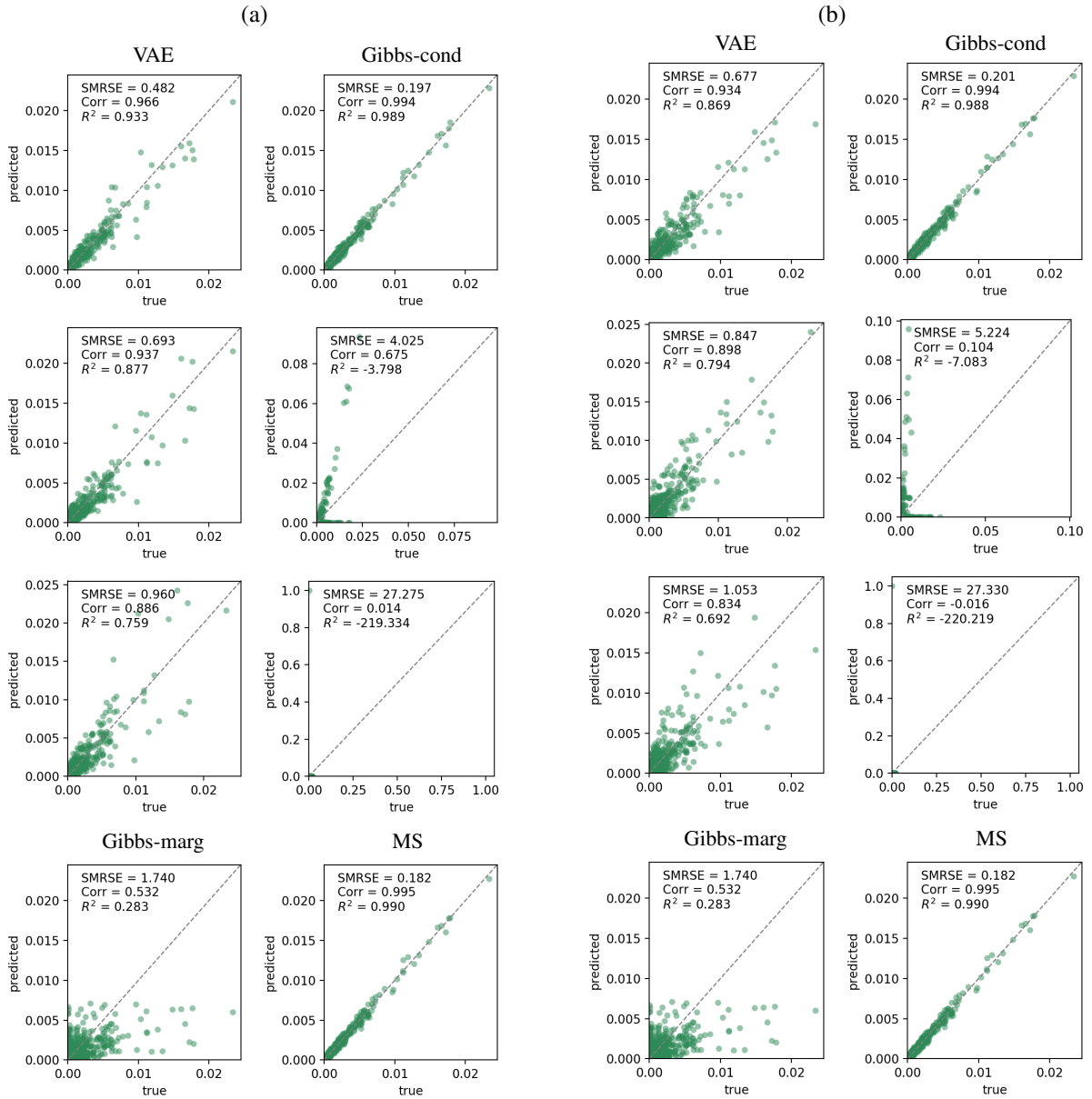


Figure 3: Comparison of the joint distributions for the true population and synthetic populations generated by VAE, Gibbs sampler for full conditionals (Gibbs-cond) and marginals (Gibbs-marg), and micro sample (MS) for the different sets of individual attributes: Basic (first row), Socio (second row) and Extended (third row). (a) numerical variables are converted to categorical and (b) without the conversion.

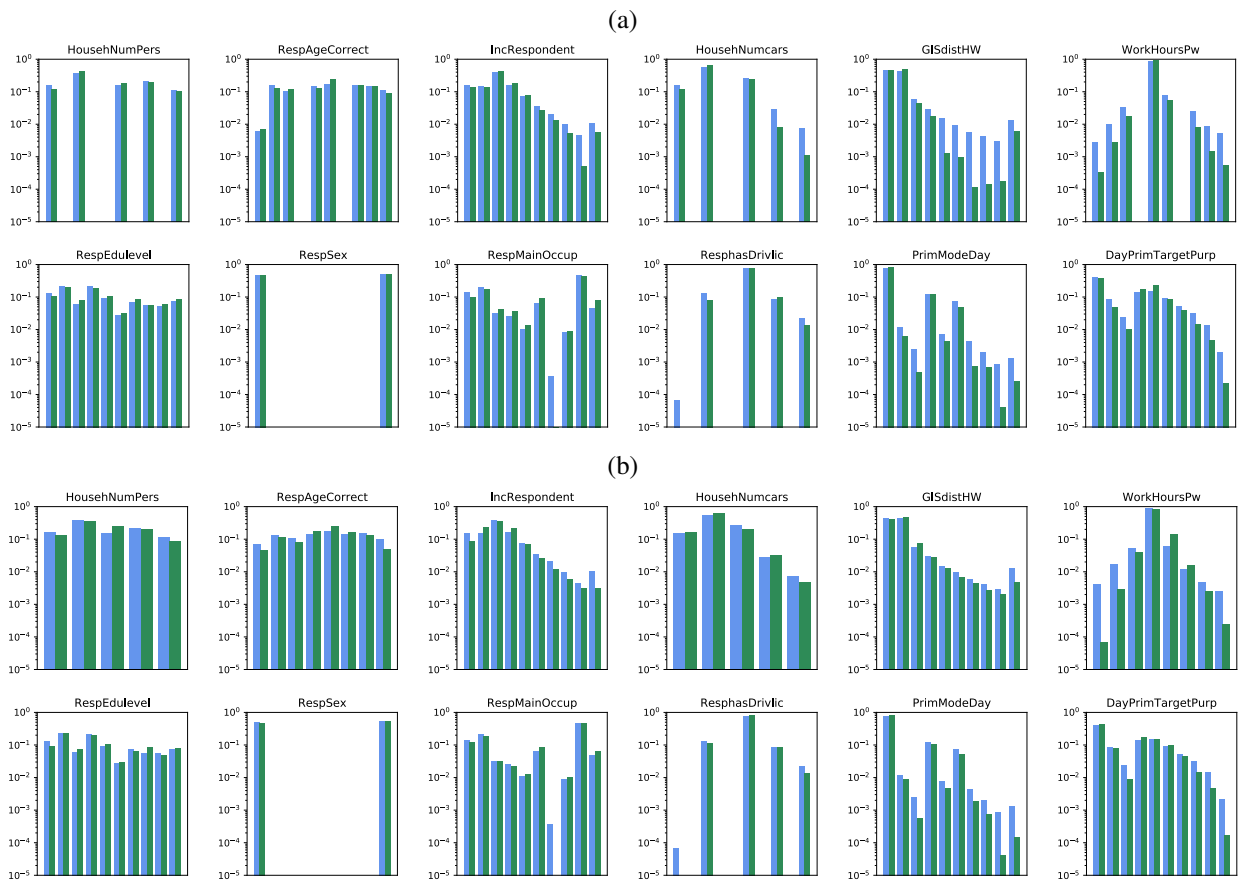


Figure 4: Examples of marginal distributions for the true population (blue) and samples generated using VAE (green) for the Extended attributes. (a) numerical variables are converted to categorical and (b) without the conversion. The first and second rows in both (a) and (b) contain numerical and categorical variables, respectively. The logarithmic scale is used to highlight low probability domains.



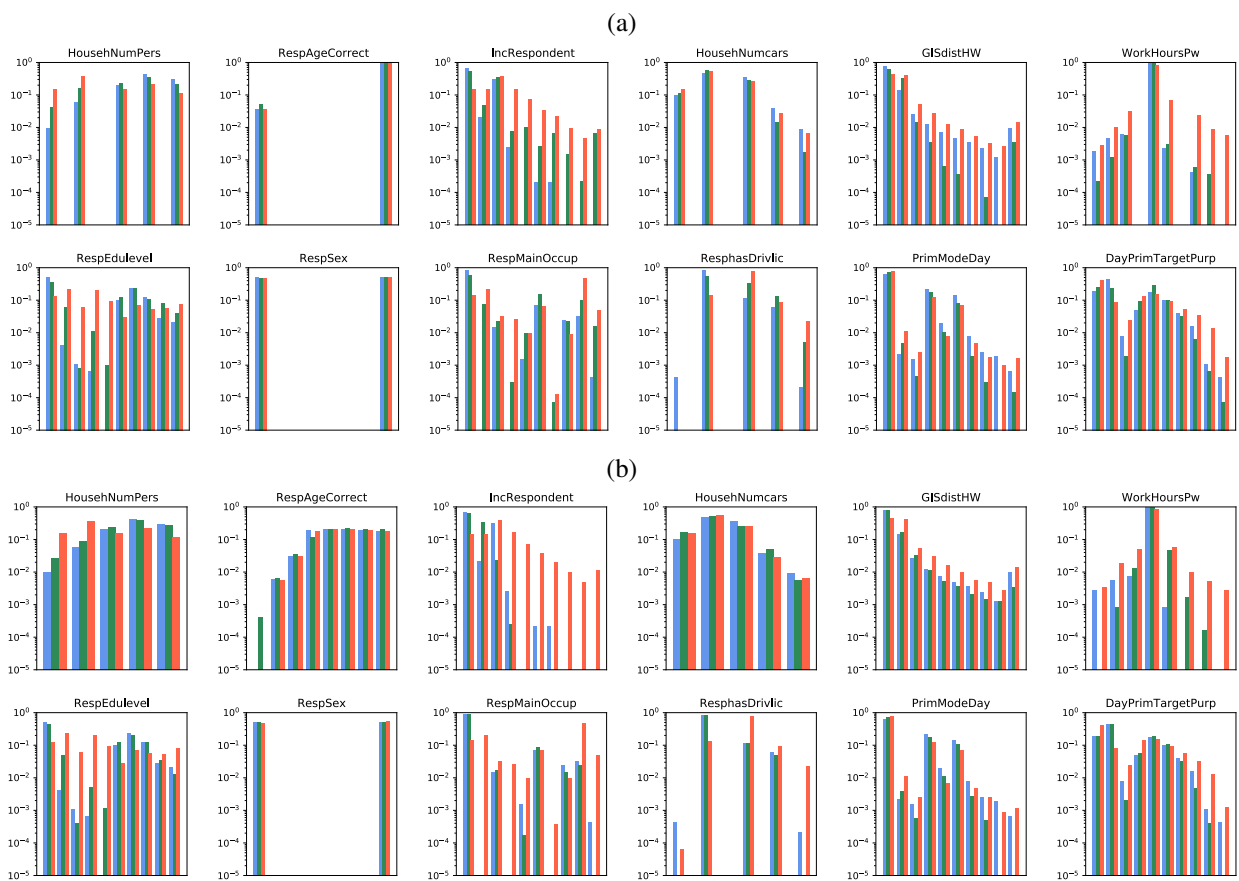


Figure 5: Examples of marginal distributions for the true population (blue), samples generated using VAE (green) and Gibbs sampler for marginals (red) for the Extended attributes for the population under 20 years old. (a) numerical variables are converted to categorical and (b) without the conversion. The first and second rows in both (a) and (b) contain numerical and categorical variables, respectively. The logarithmic scale is used to highlight low probability domains.

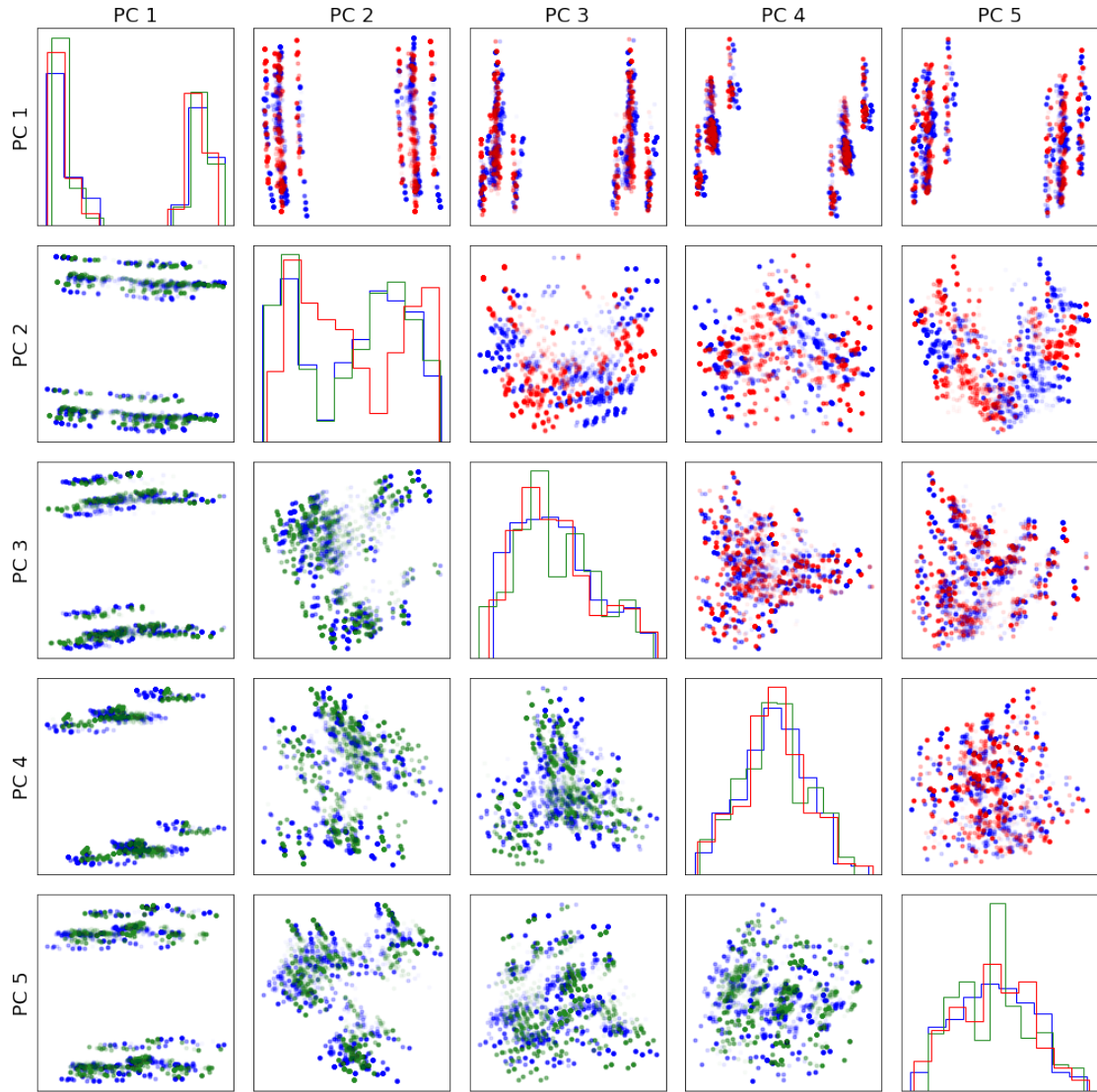


Figure 6: Principal component analysis for the Basic attributes (numerical variables are converted to categorical). The first 5 principal components (PC) of the training data (blue) and synthetic populations produced by VAE (green) and Gibbs sampling from conditionals (red) are shown. Diagonal plots show histograms of the data projected on the corresponding PC. On the off-diagonal plots, the PC data projections are plotted one against each other.

#	Name	Type	Number of values	Description
1	HousehNumPers	numerical (int)	5	Number of persons in the household
2	RespAgeCorrect	numerical (int)	8	Age
3	RespEdulevel	categorical	12	Educational attainment
4	RespSex	binary	2	Gender
5	Handicap	categorical	3	Handicap
6	HousehAccomodation	categorical	7	Home, type
7	HousehAccOwnorRent	categorical	4	Home, ownership
8	HousehNumAdults	numerical (int)	5	Number of adults in the household
9	HousehNumcars	numerical (int)	5	Number of cars in the household
10	HousehNumDrivLic	numerical (int)	5	Number of persons with driving licence in the household
11	HousehNumPers1084	numerical (int)	5	Number of persons 10-84 years in the household
12	IncHouseh	numerical (int)	10	The household's gross income
13	IncRespondent	numerical (int)	10	The respondents gross income
14	NuclFamType	categorical	5	Nuclear family type
15	PosInFamily	categorical	5	Position in the nuclear family
16	RespHasBicycle	categorical	3	Bicycle ownership
17	ResphasDrivlic	categorical	5	Driver licence
18	RespHasRejsekort	categorical	3	Danish PT smartcard
19	RespHasSeasonticket	categorical	2	Season ticket (public transport)
20	RespIsmemCarshare	categorical	3	Member of car sharing scheme
21	RespMainOccup	categorical	14	Principal occupation
22	DayJourneyType	categorical	7	Journey type of the day
23	DayNumJourneys	numerical (int)	5	Number of journeys during 24 hours
24	DayPrimTargetPurp	categorical	28	Primary stay of the day, purpose
25	DayStartJourneyRole	categorical	3	Start of the day: position in journey
26	DayStartPurp	categorical	26	Purpose at start of the day
27	GISdistHW	numerical (cont)	10	Bird flight distance between home and place of occupation
28	HomeAdrDistNearestStation	numerical (cont)	4	Home, distance to nearest station
29	HomeParkPoss	categorical	20	Parking conditions at home
30	HwDayspW	numerical (int)	7	Number of commuter days
31	HwDaysReason	categorical	8	Reason for fewer commuter days
32	JstartDistNearestStation	numerical (cont)	4	Journey base, distance to nearest station
33	JstartType	categorical	5	Journey base, type
34	ModeChainTypeDay	categorical	14	Transport mode chain for the entire day
35	NumTripsCorr	numerical (int)	4	Number of trips
36	PrimModeDay	categorical	23	Primary mode of transport for the entire day
37	RespNotripReason	categorical	7	Reason for no trips
38	TotalBicLen	numerical (cont)	6	Total bicycle travel distance
39	TotalLen	numerical (cont)	5	Total travel distance of trips
40	TotalMin	numerical (cont)	5	Total duration of trips
41	TotalMotorLen	numerical (cont)	5	Total motorised travel distance
42	TotalMotorMin	numerical (cont)	5	Total motorised duration of trips
43	WorkatHomeDayspM	numerical (int)	6	Days working from home
44	WorkHoursPw	numerical (int)	8	Number of weekly working hours
45	WorkHourType	categorical	5	Planning of working hours
46	WorkParkPoss	categorical	12	Parking conditions at place of occupation
47	WorkPubPriv	categorical	4	Public- or private-sector employee

Table 1: Individual attributes of the TU participants used in the paper. For the numerical variables, the third column denotes the number of discrete bins (i.e. categories) used for both joint distribution comparison and discretization (converting them to categorical variables). *Basic* set: attributes 1–4 (2 numerical, 2 categorical; 14-dimensional; 27-dimensional for discretized numerical). *Socio* set: attributes 1–21 (8 numerical, 13 categorical; 68-dimensional; 121-dimensional for discretized numerical). *Extended* set: attributes 1–47 (21 numerical, 26 categorical; 230-dimensional; 357-dimensional for discretized numerical).

Model	SRMSE	Corr	$R^2$	$\mu_{NS}$	$\sigma_{NS}$	SRMSE	Corr	$R^2$	$\mu_{NS}$	$\sigma_{NS}$
	Basic set (0-4/27)					Basic set (2-2/16)				
VAE	0.481	0.966	0.932	0.001	0.017	0.676	0.934	0.869	0.032	0.090
Gibbs-cond	<b>0.196</b>	<b>0.994</b>	<b>0.988</b>	0	0	<b>0.201</b>	<b>0.994</b>	<b>0.988</b>	0.033	0.098
	Socio set (0-21/121)					Socio set (8-13/68)				
VAE	<b>0.693</b>	<b>0.936</b>	<b>0.877</b>	0.004	0.035	<b>0.846</b>	<b>0.897</b>	<b>0.793</b>	0.019	0.071
Gibbs-cond	4.025	0.674	-3.798	0	0	5.224	0.103	-7.083	0.008	0.045
	Extended set (0-47/357)					Extended set (21-26/230)				
VAE	<b>0.959</b>	<b>0.885</b>	<b>0.759</b>	0.003	0.030	<b>1.184</b>	<b>0.809</b>	<b>0.609</b>	0.033	0.093
Gibbs-cond	27.27	0.014	-219.3	0	0	27.33	-0.015	-220.2	0	0
	Baselines					Baselines				
Gibbs-marg	1.740	0.532	0.283	0.037	0.094	1.740	0.532	0.283	0.037	0.094
MS	0.181	0.995	0.990	0.002	0.048	0.181	0.995	0.990	0.002	0.048

Table 2: Quality of the synthetic populations generated by VAE, Gibbs sampler for full conditionals (Gibbs-cond) and marginals (Gibbs-marg), and the micro sample used for training of the models (MS). Left/right parts of the table show the results when numerical variables are/are not converted to categorical, respectively. Columns: standardized root mean squared error (SRMSE), Pearson’s correlation coefficient (Corr) and coefficient of determination ( $R^2$ ) between the joint distributions of the synthetic and true populations.  $\mu_{NS}$  and  $\sigma_{NS}$  denote mean and standard deviation of the distances between each generated sample and its nearest sample in the training data, representing the ability of a model to generate out-of-sample agents.

Attributes Set	$n$	$D_z$	Decoder	$\beta$	$n$	$D_z$	Decoder	$\beta$
Basic	27	5	100-50-25	0.5	16	10	100-50	0.1
Socio	121	25	100	0.5	68	10	100-50-25	0.5
Extended	357	25	100	0.5	230	25	100-50	0.5

Table 3: The best VAE architectures selected using grid search. Left/right parts of the table show the results when numerical variables are/are not converted to categorical, respectively. Columns: set of attributes, dimensionality of the data space ( $n$ ), dimensionality of the latent space ( $D_z$ ), architecture of the decoding ANN, and regularization strength ( $\beta$ ). ANN architecture is denoted as “number of neurons in hidden layer 1”-“number of neurons in hidden layer 2”-... The architecture of the encoder is a mirror of the decoder.